Proceedings of the

2016 12th World Congress on Intelligent Control and Automation (WCICA)

June 12 – 15, 2016, Guilin, China

ISBN: 978-1-4673-8414-8

IEEE Catalog Number: CFP16496-ART

IEEE

Analysis of Coupling Effects between Flight and Propulsion Systems for DPC aircraft

Jing Zhang, Xianfa Zeng and Lingyu Yang

Abstract—**The noteworthy feature of aircraft with distribute propulsion configuration is the integration of the fuselage and semi-embedded distributed propulsion system, which brings strong coupling effects between flight and propulsion systems. The aim of this article is to systematically investigate the coupling effects due to boundary layer ingestion under different flight states. As the basis, the definition of boundary layer ingestion is put forward and the modeling process of distributed propulsion system is described in detail. An analysis method based on the distributed propulsion model and CFD computation is proposed. By using this method, the coupling characteristics between flight and propulsion system are generally analyzed under different flight heights and velocities. The results of this study demonstrate that the coupling effects can significantly improve the aerodynamic performance.**

I. Introduction

DISTRIBUTED propulsion configuration (DPC) is the most likely novel design of civil aircraft to effectively reduce pollution emission and improve fuel economy. Compared to the traditional large civil aircraft, the noteworthy feature of DPC aircraft is the integration of blended wing body (BWB) layout and a semi-embedded distributed propulsion system, inducing the special aerodynamic effect, i.e. boundary layer ingestion (BLI). This effect can ingest the boundary layer flow of the upper fuselage surface into engines, thus significantly improving the aerodynamic performance. On the other hand, flight and propulsion systems of DPC aircraft are strongly coupled due to the BLI effect.

The coupling effects between flight and propulsion systems are represented as two aspects: 1) Different flight states have significant influence on the intensity of boundary layer ingestion. 2) Different BLI intensities usually affect the aerodynamic characteristics of DPC aircraft.

Current researches usually focus on the specific influence of BLI effect to engine's performance. To assess the performance of BLI engines, propulsion benefits in terms of wake parameters and propulsion properties are demonstrated in [1]. The impacts of ingesting the boundary layer on the turboelectric distributed propulsion systems and off-design performance are examined in [2]. Recently numerical and experimental investigations of the BLI propulsion system are conducted[3-8], and current results show that BLI propulsors may offer power savings of up to 85% over the baseline configuration [3]. These studies usually concern about the performance of the BLI propulsion system, and limited studies are available on the coupling effects between flight and propulsion influenced by BLI. Reference [9] takes an initial investigation into the effects of boundary layer ingestion on the aerodynamic of a transonic wing. However, the DPS model is not involved in the computational procedure, thus the fidelity of computational fluid dynamics (CFD) computation would be declined consequently.

As above, as the most important feature of DPC aircraft, the coupling effects between flight and propulsion systems due to BLI should be deeply investigated. Aiming at this problem, this paper carries out a systematic research into the specific coupling effect under different flight states and its influence on the DPC aircraft's aerodynamic characteristics.

This article is organized as follows. First, the concept of BLI effect is put forward first, and then the detailed modeling process of distributed propulsion system (DPS) is given. After that, the analysis method based on DPS model and CFD is described in section Ⅲ. Then, the coupling effects between flight and propulsion systems are systematically analyzed under different flight states. Finally, analysis results and conclusions are stated.

II. Modeling of Distributed Propulsion System

A. Definition of BLI effect

For DPC aircraft, the distributed propulsion system is usually semi-embedded on the upper rear edge of the BWB fuselage, leading to the typical aerodynamic effect, BLI. The initiative purpose of BLI is to ingest the wake flow on the upper surface of fuselage into distributed engines and effectively improve fuel economy.

In this paper, the intensity of BLI η_{BLI} is defined as

$$\eta_{BLI} = \frac{A_0}{A_{01}} \tag{1}$$

where A_{01} refers to the cross-section of the engine's inlet; A_0 refers to a cross-section far ahead perpendicular to the air flow velocity with the same mass flow rate as A_{01}. The relationship between A_{01} and A_0 is shown in Fig.1.

Air mass flow rate q_m at A_{01} is expressed by

This work was supported by the National Natural Science Foundation of China under Grant No.61304030 and China Scholarship Council.

Jing Zhang is with the Science and Technology on Aircraft Control Laboratory, School of Automation Science and Electrical Engineering, Beihang University, Beijing, 100191, China (phone: 010-82316873; e-mail: zhangjing2013@buaa.edu.cn).

Xianfa Zeng is with the Beijing Institute of Control & Electronics Technology, Beijing, 100191, China (e-mail: xianfa110@163.com).

Lingyu Yang is with the Science and Technology on Aircraft Control Laboratory, School of Automation Science and Electrical Engineering, Beihang University, Beijing, China (e-mail: yanglingyu@buaa.edu.cn).

$$q_m = K\frac{P_{01}^* * A_{01} * q(\lambda_{01})}{\sqrt{T_{01}^*}} \tag{2}$$

Air mass flow rate q_m at A_0 is similarly expressed by

$$q_m = K\frac{P_0^* * A_0 * q(\lambda_0)}{\sqrt{T_0^*}} \tag{3}$$

where P^*, T^* are the total pressure and the total temperature, respectively. The subscripts "0" and "01" represent the entrance of the selected analysis region far ahead and the entrance of the inlet. K is the flow coefficient, and $q(\lambda)$ represents the flow function.

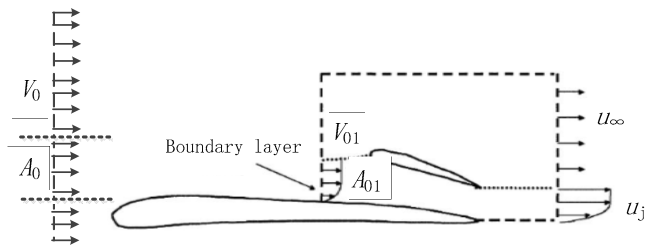

Fig. 1. Definition of the BLI intensity

According to the model characteristics of engine, we have

$$P_{01}^* = P_0^*, T_{01}^* = T_0^* \tag{4}$$

Then the intensity of BLI can be further expressed as

$$\eta_{BLI} = \frac{A_0}{A_{01}} = \frac{q(\lambda_{01})}{q(\lambda_0)} \tag{5}$$

In the above equation, the flow function $q(\lambda)$ is defined as

$$q(\lambda) = \left(\frac{\gamma+1}{2}\right)^{\frac{1}{\gamma-1}} \lambda \left(1 - \frac{\gamma-1}{\gamma+1}\lambda^2\right)^{\frac{1}{\gamma-1}} \tag{6}$$

where γ is the specific heat ratio, and λ is the velocity coefficient and it is constrained with the Mach number Ma as below

$$\lambda^2 = \frac{\frac{\gamma+1}{2}Ma^2}{1+\frac{\gamma+1}{2}Ma^2} \tag{7}$$

B. Modeling process of DPS

As the most representative aircraft with distributed propulsion configuration, SAX-40 is selected as the research object in this paper. The distributed propulsion system of SAX-40 is composed of three distributed engines. Each engine has three separated tunnels in which a turbofan mainly provides engine thrust. The control parameters of each engine can be adjusted individually. The simplified structure of each engine is shown as Fig.2.

As the inherent characteristics of each tunnel is same, the modeling process of one tunnel is described as follows.

1) Characteristic equations of components

The thermodynamic process of each component formulates the following assumptions: (1) The pre-compression segment is an adiabatic process. (2) There is a loss of total pressure in the inlet and convergent nozzle respectively, and it can be represented by the total pressure recovery coefficient.

According to the thermodynamic process, characteristic equations of the components in each tunnel can be derived as bellow [10]:

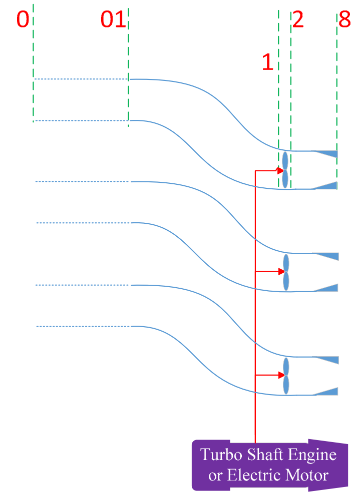

Fig. 2. Components of each engine

Explanations: "0" represents the area located in the undisturbed airflow far ahead; "01" represents the entrance of the inlet; "1" and "2" represent the front and rear section of the fan respectively; "8" represents the exit of the nozzle. The area between section "0" and "01" is pre-compression segment; the component between "01" and "1" is inlet; the turbofan and nozzle are located between sections "1" and "2", "2" and "8" respectively.

a) Pre-compression segment: $P_{01}^* = P_0^*, T_{01}^* = T_0^*$

b) Inlet: $P_1^* = \sigma_i * P_{01}^*$, $T_1^* = T_{01}^*$

c) Fan: $P_2^* = \pi_k^* * P_1^*$, $T_2^* = T_1^* * \left(\pi_k^*\right)^{\frac{\gamma-1}{\gamma}}$

d) Nozzle: $P_8^* = \sigma_e * P_2^*, T_8^* = T_2^*$

where σ_i, σ_e are the total pressure recovery coefficients of the inlet and the nozzle, respectively. Numbers in the subscripts represent the corresponding sections in Fig.2.

2) Supplementary equations

As described in (2) and (3), the air mass flow rate at inlet and outlet of each tunnel satisfies

$$q_m = K\frac{P_{01}^* * A_{01} * q(\lambda_{01})}{\sqrt{T_{01}^*}} = K\frac{P_8^* * A_8 * q(\lambda_8)}{\sqrt{T_8^*}} \tag{8}$$

where A_8 refers to the nozzle exit area.

Furthermore, the compressed air at A_8 should be checked whether it fully expands, and the corresponding expressions satisfy

$$\begin{cases} q(\lambda_8) = 1 & \beta_8 = \dfrac{P_0}{\sigma_e * \sigma_i * \pi_k^* * P_0^*} < \left(\dfrac{2}{\gamma+1}\right)^{\frac{\gamma}{\gamma+1}} \\ P_8 = P_0 & \beta_8 = \dfrac{P_0}{\sigma_e * \sigma_i * \pi_k^* * P_0^*} > \left(\dfrac{2}{\gamma+1}\right)^{\frac{\gamma}{\gamma+1}} \end{cases} \tag{9}$$

where P is the static pressure.

3) Thrust and power consumption

With the air velocity V_0, V_8 at the inlet and exit of each tunnel, the thrust F and power consumption P_{re} can be obtained as

$$\begin{cases} F = q_{m0} * (V_8 - V_0) + A_8 * (P_8 - P_0) \\ P_{re} = q_{m0} * w_k \end{cases} \tag{10}$$

where $w_k = \frac{\gamma}{\gamma - 1} R * T_0^* * \left[\left(\pi_k^* \right)^{\frac{\gamma-1}{\gamma}} - 1 \right] / \eta_k^*$ means the power consumption with unit air mass flow rate; R is the gas constant, η_k^* is the efficiency of power transmission.

As above, the mathematical model of each tunnel is built. By synthesizing the feature equations of all tunnels, a whole DPS model can be obtained. This model can provide essential boundary conditions for CFD computation.

III. Analysis Method Based on DPS Model

According to the boundary conditions provided by the DPS component model, an analysis method based on the DPS model and CFD is described in this section. In this method, a synthetic 2D computational model is designed to simulate the boundary layer ingesting process by using the boundary section parameters, which are designated by the DPS model.

First, as the basis, a whole shape model including fuselage and propulsion are built in the CFD environment. As the BLI effect mainly occurs in the entrance of distributed engines, a representative 2D model is captured at the longitudinal section including the left engine. The whole shape model and 2D computational model are illustrated in Fig.3.

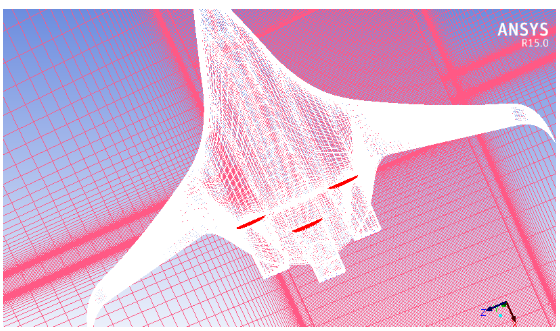

(a) whole shape model

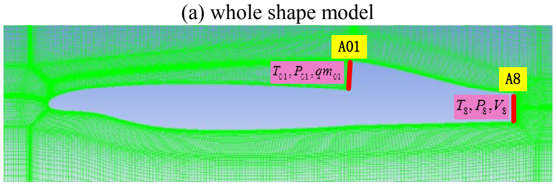

(b) 2D section model with engine

Fig. 3. CFD computation model

The 2D section model is mainly used to compute and analyze the BLI effect, and the whole model can validate the effectiveness and guarantee the accuracy of the computational model. In the 2D section model, the boundary section parameters contain engine's entrance parameters including the static temperature T_{01}, the static pressure P_{01}, the flow rate q_{m01}, as well as engine's outlet parameters including the static temperature T_8, the static pressure P_8, the jet velocity V_8. These boundary parameters can be calculated by the DPS mathematic model.

By changing the parameters (T_{01}, P_{01}, q_{m01}), (T_8, P_8, V_8) of DPS at different flight states, the coupling effects between flight and propulsion systems can be simulated and computed by CFD computation, and consequently the influence regularity of the BLI effect on aerodynamic characteristics can be determined.

IV. Analysis and Results

Based on the DPS model and CFD computation, coupling effects between flight and propulsion system are investigated. Analyses of the BLI effect under different flight states and its direct influence on aerodynamic characteristics are conducted in this section.

A. *Analysis of coupling effects under different velocities*

Typical flight height $H = 10000m$ and different velocities $Ma = 0.6$, $Ma = 0.8$ are selected for comparisons. By computing with CFD, the velocity and pressure plots of 2D model with BLI effect at $H = 10000m$, $Ma = 0.6$ are obtained, as shown in Fig.4.

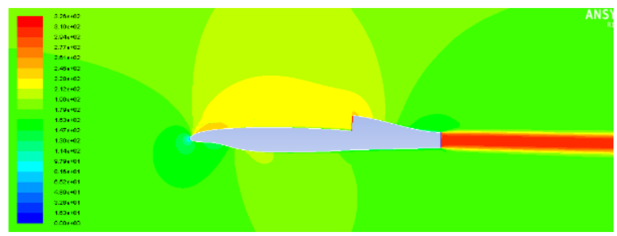

(a) velocity plot of the intact section

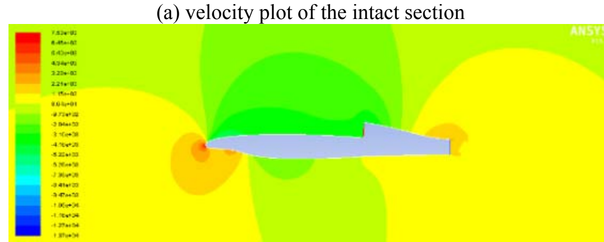

(b) pressure plot of the intact section

Fig. 4. Velocity and pressure plots under H=10000m, Ma=0.6

In comparison, the velocity and pressure plots at the same height and $Ma = 0.8$ are obtained, as shown in Fig.5.

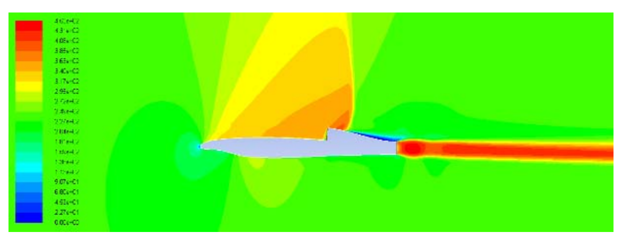

(a) velocity plot of the intact section

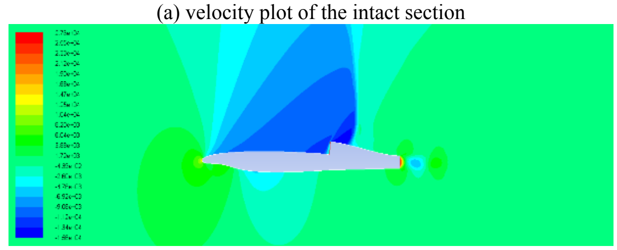

(b) pressure plot of the intact section

Fig. 5. Velocity and pressure plots under H=10000m, Ma=0.8

As shown in Fig.4 and 5, we can discover that a shock wave emerges on the upper surface at high speed $Ma = 0.8$, and consequently a low-pressure region occurs on the entrance of the nacelle.

With different BLI intensities, the lift coefficient C_l at different flight velocities are shown in Fig.6.

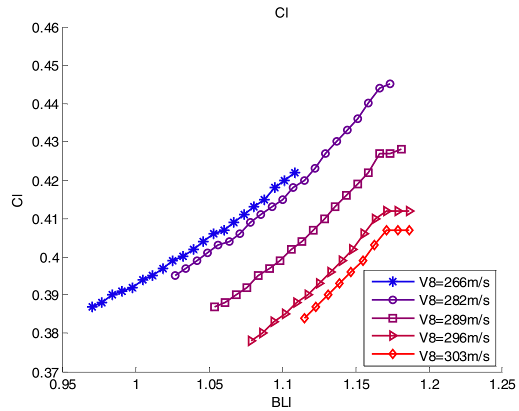

(a) the lift coefficient at H=10000m, Ma=0.6

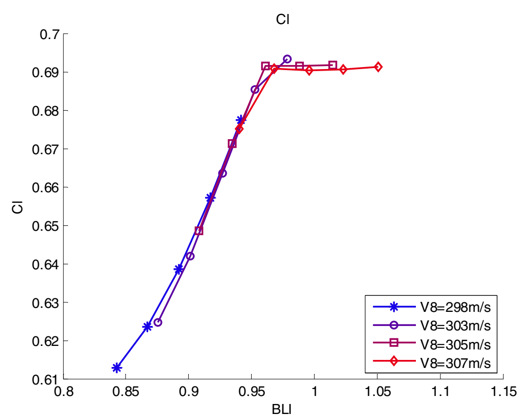

(b) the drag coefficient at H=10000m, Ma=0.8

Fig. 6. Comparisons of aerodynamic coefficients at different velocities

As can be seen in Fig.6, the BLI effect can significantly affect aerodynamic characteristics. With BLI effect increasing, the lift coefficient increases sharply and then reaches a limit at the certain extent of BLI intensity. Comparisons between different velocities $Ma = 0.6$, $Ma = 0.8$ reveals that the lift coefficient at $Ma = 0.8$ is generally larger than the lower speed, which is coordinated with the CFD computation results shown in Fig.4 and Fig.5. Likewise, the variation range inducing by BLI effect is larger at high speed, which indicates that the improvement to aerodynamic lift of BLI effect would be enhanced.

B. *Analysis of coupling effects under different heights*

Another typical flight state $H = 5000m$, $Ma = 0.6$ is selected to analyze aerodynamic characteristics under various heights. The velocity and pressure plots of 2D model with BLI effect at $H = 5000m$, $Ma = 0.6$ are shown in Fig.7. Under this flight state, the lift coefficient C_l with different BLI intensities is shown in Fig.8.

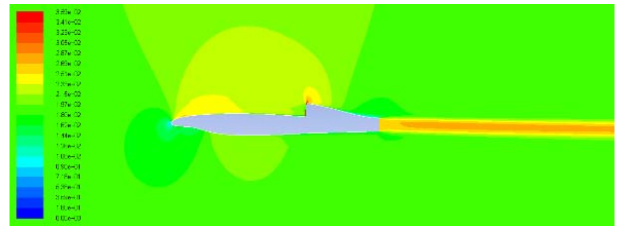

(a) velocity plot of the intact section

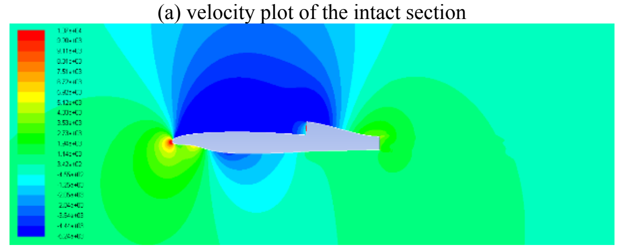

(b) pressure plot of the intact section

Fig. 7. Velocity and pressure plots under H=5000m, Ma=0.6

By comparison to results at former height $H = 10000m$, we can find that the airflow velocity in the entrance of the inlet is lower at height $H = 5000m$, and another feature is a lower jet velocity required due to more airflow ingested into engines.

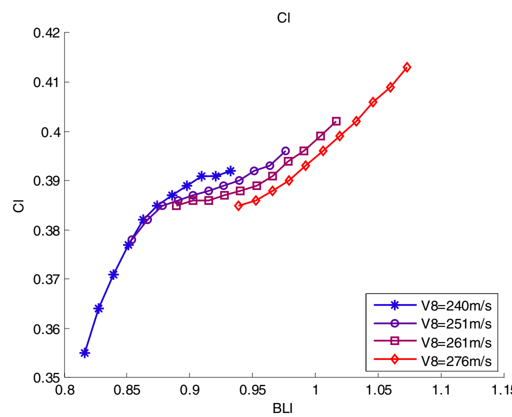

Fig. 8. Aerodynamic lift coefficient under H=5000m, Ma=0.6

Compared to aerodynamic characteristics at $H = 10000m$, $Ma = 0.8$, the common feature of the lift coefficient C_l is that it will increase along with the intensifying BLI effect. However, the differences are also obvious. First, the curves distribute more tightly at the lower height, meaning that the inducing effect of jet velocity is weaker at $H = 5000m$. Moreover, the lift coefficient varies linearly throughout the entire BLI intensity range at $H = 10000m$. However, there is a slow-varying region $\eta_{BLI} \in [0.9,1.0]$ on the C_l curve at $H = 5000m$, meaning that there is a retardation region as the height is lower.

In conclusion, different flight states including velocity and height have significant influence on the intensity of boundary layer ingestion, forming variation pressure distribution of airflow on the upper surface of fuselage, and this leads to a further impact on the aerodynamic characteristics of DPC aircraft.

V. Conclusion

The coupling effect between flight and propulsion systems is an important feature of DPC aircraft. Aiming at this point, this article presents a systematic research into the specific coupling effect under different flight states. The regularities of coupling effects are calculated based on the DPS model and CFD computation.

A point to be taken into further consideration is the comprehensive analysis method based on 3D computational model. Compared to the 2D computational model in this article, 3D model including the fuselage and all distributed engines can generate more accurate computational results. Furthermore, the lateral aerodynamic characteristics due to discrepant BLI effects can also be analyzed, which is essential to realize integrated control of DPC aircraft.

Acknowledgment

Authors acknowledge the research object derived from the Silent Aircraft Initiative program conducted by Cambridge University and MIT.

References

[1] L.H. Smith, "Wake ingestion propulsion benefit," *Journal of propulsion and power*, vol.9, pp.74-82, 1993.

[2] J.L. Felder, H.D. Kim, G.V. Brown, et al, "An examination of the effect of boundary layer ingestion on turboelectric distributed propulsion systems," in *Proc. 49th AIAA Aerospace Sciences Meeting including the New Horizons Forum and Aerospace Exposition* , Orlando, Florida, 2011, pp. 1–26.

[3] A.A. Elmiligui, W.J. Fredericks, M.D. Guynn, et al, "Numerical investigation of a fuselage boundary layer ingestion propulsion concept," in *Proc. Aviation Technology, Integration and Operations Conference*, Los Angeles, CA, 2013, pp. 1–18.

[4] O. Atinault, G. Carrier, R. Grenon, et al, "Numerical and experimental aerodynamic investigations of boundary layer ingestion for improving propulsion efficiency of future air transport," in *Proc. 31st AIAA Applied Aerodynamics Conference*, San Diego, CA, 2013, pp. 1–13.

[5] K. Sabo, M. Drela, "Benefits of boundary layer ingestion propulsion," in *Proc. 53rd AIAA Aerospace Sciences Meeting*, Kissimmee, Florida, 2015, pp. 1–14.

[6] S.S. Ochs, G. Tillman, J. Joo, D.M.Voytovych, "CFD-based analysis of boundary layer ingesting propulsion," in *Proc. 51st AIAA/SAE/ASEE Joint Propulsion Conference*, Orlando, Florida, 2015, pp. 1–15.

[7] H.J. Kok, M. Voskuijl, M.J. Tooren, "Distributed propulsion featuring boundary layer ingestion engines for the blended wing body subsonic transport," in *Proc. 51st AIAA/ASME/ASCE/AHS/ASC Structures, Structural Dynamics and Materials Conference*, Orlando, Florida, 2010, pp. 1–12.

[8] A. Plas, "Performance of a boundary layer ingesting propulsion system," M.S. thesis, Dept. of Aeronautics and Astronautics, Massachusetts Institute of Technology, Cambridge, US, 2006.

[9] V.M. Lugo, G. Doulgeris, R. Singh, "Computational analysis of the effects of a boundary layer ingesting propulsion system in transonic flow," *Proc IMechE Part G: Journal of Aerospace Engineering*, vol.227, pp.1215-1232, 2012.

[10] W.W. Kang, J. Zhang, L.Y. Yang, "Research on boundary layer ingestion effects of distributed propulsion configuration," in *Proc. 2014 IEEE Chinese Guidance, Navigation and Control Conference*, Yantai, China, 2014, pp. 1–8.